New Superfamily Members Identified for Schiff-Base Enzymes Based on Verification of Catalytically Essential Residues†

Kyung H. Choi,‡,§ Vicky Lai,§ Christine E. Foster,§ Aaron J. Morris,§ Dean R. Tolan,*,§ and Karen N. Allen*,‡

Department of Biology, Boston University, 5 Cummington Street, Boston, Massachusetts 02215, and Department of Physiology and Biophysics, Boston University School of Medicine, 715 Albany Street, Boston, Massachusetts 02118-2394

Received February 5, 2006; Revised Manuscript Received May 16, 2006

ABSTRACT: Enzymes that utilize a Schiff-base intermediate formed with their substrates and that share the same α/β barrel fold comprise a mechanistically diverse superfamily defined in the SCOPS database as the class I aldolase family. The family includes the "classical" aldolases fructose-1,6-(bis)phosphate (FBP) aldolase, transaldolase, and 2-keto-3-deoxy-6-phosphogluconate aldolase. Moreover, the *N*-acetylneuraminate lyase family has been included in the class I aldolase family on the basis of similar Schiff-base chemistry and fold. Herein, we generate primary sequence identities based on structural alignment that support the homology and reveal additional mechanistic similarities beyond the common use of a lysine for Schiff-base formation. The structural and mechanistic correspondence comprises the use of a catalytic dyad, wherein a general acid/base residue (Glu, Tyr, or His) involved in Schiff-base chemistry is stationed on β-strand 5 of the α/β barrel. The role of the acid/base residue was probed by site-directed mutagenesis and steady-state and pre-steady-state kinetics on a representative member of this family, FBP aldolase. The kinetic results are consistent with the participation of this conserved residue or position in the protonation of the carbinolamine intermediate and dehydration of the Schiff base in FBP aldolase and, by analogy, the class I aldolase family.

The definition of enzyme superfamilies has provided insights into structure−function relationships for enzymes. These relationships have helped reveal mechanistic similarities among enzymes that must perform difficult chemistry based on the premise that nature most often does not need to find two ways to catalyze a common reaction. Enzymes of such "mechanistically diverse superfamilies" (*1*, *2*) often have very low pairwise sequence identity and conserved active-site elements that perform the common mechanistic function for all members of the superfamily and exhibit the same general fold.

Often, the common chemistry is all that is left of mechanistically diverse enzymes that shared a common ancestor. This feature has been used to define a number of enzyme superfamilies (*3*). Those enzymes that utilize a Schiff-base intermediate formed with the substrate and have the same fold may comprise one such mechanistically diverse superfamily and have been defined as such in the SCOPS database (*4*) as the class I aldolase family. Members of this superfamily, exemplified by the glycolytic enzyme fructose-1,6-(bis)phosphate aldolase (FBPA,[1] EC 4.1.2.13), have long been known to utilize a Schiff base and are among the many enzymes with an $(\alpha/\beta)_8$ barrel fold. FBPA catalyzes the cleavage of fructose 1,6-(bis)phosphate (Fru-1,6-P_2) into two trioses, glyceraldehyde 3-phosphate (G-3-P) and dihydroxyacetone phosphate (DHAP). Fru-1,6-P_2 aldolases are divided into two classes on the basis of their reaction mechanisms (*5*). Class I aldolases catalyze the reaction through a Schiff-base intermediate between the active-site lysine and the carbonyl carbon of the substrate and are found in most eukaryotes and archaebacteria (*6*, *7*). Class II aldolases require a metal cation for catalysis, which polarizes the carbonyl oxygen of the substrate, and are found in eubacteria and fungi. Although both classes have a similar $(\alpha/\beta)_8$ barrel fold (*8*, *9*), class II aldolases are not part of the Schiff-base aldolase superfamily. Other class I Schiff-base aldolases include transaldolase (TRANS), 2-keto-3-deoxy-6-phosphogluconate aldolase (KDPGA), and deoxyribose phosphate aldolase (DRPA).

† This work was supported by National Institutes of Health Grants DK43521 and DK065089 (to D.R.T.) and GM60616 (to D.R.T. and K.N.A.). It was also supported in part by a National Institutes of Health grant for Research Experience for Undergraduates (to V.L.).

* To whom correspondence should be addressed. K.N.A.: Department of Physiology and Biophysics, 715 Albany St., Boston University School of Medicine, Boston, MA 02118; phone, (617) 638-4398; fax, (617) 638-4273; e-mail, allen@med-xtal.bu.edu. D.R.T.: Biology Department, 5 Cummington St., Boston, MA 02215; phone, (617) 353-5310; fax, (617) 358-0338; e-mail, tolan@bu.edu.

‡ Boston University School of Medicine.

§ Boston University.

[1] Abbreviations: Fru-1,6-P_2, fructose 1,6-(bis)phosphate; Fru-1-P, fructose 1-phosphate; DHAP, dihydroxyacetone phosphate; G-3-P, glyceraldehyde 3-phosphate; SDS, sodium dodecyl sulfate; PAGE, polyacrylamide gel electrophoresis; MOPS, 3-(*N*-morpholino)propanesulfonic acid; TEA, triethanolamine; TAPS, *N*-tris(hydroxymethyl)-methyl-3-aminopropanesulfonic acid; rmsd, root-mean-square deviation; MES, 2-(*N*-morpholino)ethanesulfonic acid; Tris, tris(hydroxymethyl)-aminomethane; EDTA, ethylenediaminetetraacetic acid; NADH, reduced nicotinamide adenine dinucleotide; BSA, bovine serum albumin; FBPA, fructose-1,6-bisphosphate aldolase; TRANS, transaldolase; KDPGA, 2-keto-3-deoxy-6-phosphogluconate aldolase; DRPA, deoxyribose phosphate aldolase; NAL, *N*-acetylneuraminate lyase; DHDPS, dihydrodipicolinate synthase; DQD, 3-dehydroquinate dehydratase.

10.1021/bi060239d CCC: $33.50
Published on Web 06/27/2006

Table 1: Enzymes and Reactions of the Aldolase Superfamily

family member	PDB entry	abbreviation	"covalent" substrate[a]	second substrate	face[b]	β-K[c]	β-A/B[d]
Fru-1,6-P_2 aldolase	1ADO	FBPA	DHAP	G-3-P	*si*	6	5
transaldolase	1ONR, 4PER	TRANS	fructose 6-phosphate	erythrose 4-phosphate	—[e]	6[f]	5
2-keto-3-deoxy-6-phosphogluconate aldolase	1EUA	KDPGA	pyruvate	G-3-P	*si*	6	2
2-deoxyribose-5-phosphate aldolase	1JCJ	DRPA	acetaldeyhyde	G-3-P	*si*	6	X[g]
N-acetylneuraminate lyase	1NAL, 1FDY	NAL	pyruvate	*N*-acetylmannosamine	*si*	6	5
dihydrodipicolinate synthase	1DHP	DHDPS	pyruvate	aspartate β-semialdehyde	—[e]	6	5
3-dehydroquinate dehydratase	1QFE	DQD	pyruvate	salicylaldehyde	—[e]	6	5

[a] The substrate that forms the Schiff base. [b] Determination of *si*-face attack is inferred from the configuration of the resulting (*R*)-carbinolamine (*11*, *40*, *41*) or from the resulting reduced lysines (*51*). [c] The β-strand from which the Schiff-base-forming lysine arises. [d] The β-strand from which the acid/base catalyst for Schiff-base formation arises. [e] Not determined. [f] For TRANS [and fructose-6-phosphate aldolase (*50*)], there is evidence that a two-strand circular permutation of the β-barrel has occurred (*52*). In the native protein, the residues of the catalytic dyad are from strands 4 and 3, respectively (*52*). [g] A structured water is proposed to act as an acid/base catalyst (*41*). In DRPA, the water is liganded to residues C47, D16, T18, D102, and K137.

Another group of enzymes utilizing a Schiff-base intermediate that have been described as comprising a homologous family (*10*) includes *N*-acetylneuraminate lyase (NAL), dihydrodipicolinate synthase (DHDPS), and 3-dehydroquinate dehydratase (DQD). All three proteins share the same $(\alpha/\beta)_8$ barrel fold and perform a reverse aldol condensation using a Schiff-base intermediate. The definition of the NAL family was based on sequence and structural similarities quantified by database searches and computational fitting of secondary structure motifs to a template model (*11*). The NAL family has been included in the class I aldolase family by the SCOPS database only on the basis of similar Schiff-base chemistry and fold (*4*). The names, abbreviations, reactions, substrates, and active-site residues for the class I aldolase family are given in Table 1. The level of sequence similarity between family members is much less than 10%, based on primary sequence alignment. Herein, we generate primary sequence identities based on the structural alignment, which support the homology and reveal additional mechanistic similarities beyond the common use of a lysine for Schiff-base formation.

The catalytic mechanism of class I aldolase has been extensively studied using FBPA from rabbit muscle. On the basis of the experimental data (*12*−*15*), it is clear that the aldol cleavage proceeds through a number of distinct steps, including a ring opening (*16*), and carbinolamine, imine (Schiff-base), and enamine/carbanion formation as shown in eq 1:

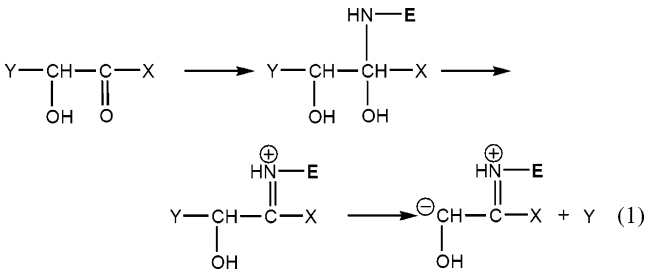

(1)

where for the reaction catalyzed by FBPA, X is $CH_2PO_4^{2-}$ (as part of the "covalent" substrate delineated in Table 1), Y is $C_3H_6O_2PO_4^{2-}$ (as part of the second substrate delineated in Table 1), and E is the enzyme. Following ring opening, a lysine residue in the active site (Lys229) attacks the carbonyl carbon of the substrate, leading to a carbinolamine followed by dehydration to form a Schiff base. Subsequent cleavage of the C3−C4 bond releases G-3-P or glyceraldehyde depending on the substrate and leaves the product enamine/carbanion bound at the active site. Protonation of the carbanion and hydrolysis of the resultant Schiff base release the second product, DHAP, and regenerate the enzyme (*17*, *18*). We posit that essential residues involved in formation and hydrolysis of the Schiff-base intermediate would be conserved in all mechanistically diverse superfamily members. In a superfamily, the positions of such residues should be contributed from the same secondary structure elements (*19*).

In FBPA, the identification of the general acid/bases involved in Schiff-base formation has been performed by a combination of site-directed mutagenesis, kinetics, and X-ray crystallography (*18*, *20*−*23*). The structure of the Schiff base of DHAP trapped on the enzyme by $NaBH_4$ revealed the proximity of Glu187 to C2 in the DHAP structure (*20*). The noncovalently liganded structure with DHAP (*24*) revealed the proximity of Glu187 to Lys229. These data indicate that this residue could act as the general acid protonating the carbinolamine intermediate and thus catalyzing dehydration to the Schiff base. The proposed role is supported by two recently reported structures of a cryo-captured Schiff-base intermediate of FBP in FBPA (*25*) and a trapped carbinolamine in a class I FBPA from archaebacteria (*26*). The structures of several aldolases substituted at Glu187 show few perturbations except at the site of the substitution (*27*). Analysis of steady-state intermediates and kinetic values of these Glu187-substituted enzymes have suggested that Glu187 may act either as the general base initiating C−C bond cleavage or in steps preceding the cleavage reaction, including Schiff-base formation (*25*, *27*). Structural analysis of several Schiff-base aldolases with covalently bound ligands has suggested that Glu187 along with the Schiff-base-forming lysine comprises a "catalytic dyad" (*20*).

In this report, the steady-state and pre-steady-state kinetics of FBPA with substitutions of Ala, Gln, Ser, and Asp at Glu187 were analyzed. The results showed that the largest change was in the rate of Schiff-base formation and not C−C bond cleavage, thus supporting a single role for this residue as a general acid catalyst in the formation of the Schiff base. Such a central role for Glu187 suggested that a residue would be stationed in the same position in other family members utilizing the same chemistry with similar stereoconstraints on substrates. To assess whether there may be an evolution-

ary or mechanistic link between the classic aldolases and the NAL family, structural alignment of all members was performed. This analysis revealed a significant similarity in primary sequence alignments based on structural alignments and identified a catalytic acid/base (His or Tyr) contributed by the same β-strand as Glu187 in the FBPA. Comparison of the primary and tertiary structures of these enzymes to other α/β barrel enzymes was consistent with their inclusion in a large superfamily utilizing Schiff-base chemistry and related by divergent evolution from a common progenitor.

MATERIALS AND METHODS

Materials. Fru-1,6-P_2, Fru-1-P, and other chemicals were from Sigma-Aldrich (St. Louis, MO). CM-Sepharose CL-6B Fast Flow was purchased from Pharmacia LKB Biotechnology Inc. Radiolabeled [U-^{14}C]Fru-1,6-P_2 was from ICN. Scintillation fluid (Aquasol) was from Dupont. Thin-layer chromatography plates were from Whatman. SDS low-molecular weight standards were from Bio-Rad. Enzymes for site-directed mutagenesis were from New England Biolabs (Ipswich, MA). Oligodeoxyribonucleotides for site-directed mutagenesis and DNA sequencing were synthesized on a Milligen/Biosearch DNA synthesizer using phosphoramidite chemistry and the manufacturer's protocols.

Construction of the Expression Plasmid. The Glu187 substitutions were created in *Escherichia coli* strain TG1 (*28*) containing M13-derived DNA. The site-directed mutagenesis was performed to change the Glu187 codon to the Ala, Asp, Gln, or Ser codon using the oligodeoxyribonucleotide 5′-CCATTGTGNNNCCCGAAATC-3′, where NNN was GCG, GAC, CAG, and TCG for Ala, Asp, Gln, and Ser, respectively. M13-derived AM1 (*22*), encoding rabbit aldolase A cDNA, was used as a template for site-directed mutagenesis (*29*). Single-stranded DNA was prepared from resulting phage plaques. DNA sequencing confirmed the presence of the mutation and that no accidental changes in the sequence were introduced. The RF form of the M13 clones was used to subclone an *Eco*RI−*Hin*dIII fragment containing the entire aldolase open reading frame into pPB1 (*30*) and the recombinant plasmid transformed into *E. coli* strain DH5α (*31*).

Purification of Recombinant Aldolase. Wild-type and Glu187-substituted FBPA were expressed in *E. coli* and purified as previously described (*22*). Briefly, the crude extract was cleared and then centrifuged again at 100000*g*. The 35−65% ammonium sulfate fraction was dialyzed and loaded onto a CM-Sepharose CL-6B Fast Flow column equilibrated with MGK buffer [50 mM MOPS·glycine·KOH (pH 7.0) and 1 mM dithiothreitol]. The column was washed with TGK buffer [50 mM TAPS·glycine·KOH (pH 8.3) and 1 mM dithiothreitol], and the FBPA eluted with TGK buffer containing 2 mM Fru-1,6-P_2. The fractions with FBPA activity were pooled, precipitated with 75% saturated ammonium sulfate, and stored at 4 °C.

Kinetic Analysis. Aliquots of the protein precipitated with ammonium sulfate were dialyzed against 5 mM TEA-HCl (pH 7.4) and 1 mM dithiothreitol for use in kinetic assays. The substrate cleavage rate was determined in triplicate using a coupled assay for oxidation of NADH as described previously (*22*, *32*). The cleavage rates for Fru-1,6-P_2 were measured over a substrate range of 1.25−160 μM, with 0.5 μg of wild-type enzyme or 100 μg to 1 mg of Glu187-substituted protein. The cleavage rate of Fru-1-P was measured over a substrate range of 3.0−50 mM, with 5 μg of wild-type enzyme or 300 μg to 1 mg of mutant enzymes. Kinetic values were determined from double-reciprocal plots using the least-squares method of Cleland (*33*). The protein concentration was determined by absorbance using an E_{280}-(0.1%) of 0.91 (*34*).

Pre-Steady-State Kinetic Measurement. Reactions were started by rapidly mixing 15 μL of [U-^{14}C]Fru-1,6-P_2 (295 Ci/mol) and 15 μL of enzyme in 10 mM Tris-HCl (pH 7.4) to final concentrations of 2.5 and 32.5 μM, respectively. No significant differences in kinetic values were observed when the substituted enzymes were varied in concentration from 7- to 50-fold in excess of substrate. The solution was incubated at 22 °C for 2−3000 s and the reaction quenched with 2 N HCl. The quenched reaction solution was centrifuged for 1 min, and the supernatant fraction was removed and saved. The centrifuge tube containing the precipitated protein was rinsed with 100 μL of cold 2 N HCl and lyophilized. The rinse solution was combined with the supernatant fraction and lyophilized. The amount of radiolabeled Fru-1,6-P_2 incorporated into the precipitated enzyme was determined by adding scintillation fluid to the dried precipitant and counting in a Beckman LS 2800 scintillation counter. The counting efficiency was 90%. For wild-type FBPA, the reactions were performed at 4 °C in a KinTek Instruments quench-flow apparatus with a reaction time of 3−1000 ms.

The substrate and products in the supernatant fraction were quantified by thin-layer chromatography. The fractions were resuspended in water and applied (33%) to a silica plate, and the plate was developed using 1-butanol, glacial acetic acid, and water (5:3:2). Amounts were measured with a Bio-Rad Phosphorimager by cochromatography of [U-^{14}C]Fru-1,6-P_2 at known concentrations. To ensure that the acid was quenching the enzymatic reaction, a control reaction mixture of enzyme added to premixed acid and substrates was included in each experiment. Control experiments were also performed to check the stability of the substrates under the quench conditions and to determine the background of the assay.

Data Analysis. The single-turnover kinetic values were determined as described previously using an irreversible reaction depicted in eq 2 (*18*):

$$\text{E} + \text{Fru-1,6-P}_2 \xrightarrow{k_1} \text{E}{=}\text{Fru-1,6-P}_2 \xrightarrow{k_2} \text{G-3-P} + \text{DHAP} + \text{E} \quad (2)$$

where E=Fru-1,6-P_2 is the Schiff-base intermediate whose rate of formation is k_1. The rate constant k_1 represents the combination of several rates: bimolecular binding, the unimolecular conversion of the bound enzyme−substrate complex to the first covalent carbinolamine intermediate, the conversion of this carbinolamine to the Schiff base, and any dissociation reaction. The model assumes that the rates of association and dissociation are fast compared to the rate of formation of covalent intermediates under the pre-steady-state conditions. The intermediate termed the Schiff base in eq 2 refers to both the carbinolamine and the imine since both are stable in the acid precipitate (*35*). The rate of

Table 2: Steady-State Rates of Fru-1,6-P_2 and Fru-1-P Cleavage for Glu187 Substitutions in FBPA

	Fru-1,6-P_2				Fru-1-P			
aldolase	k_{cat} (s^{-1})	Δ	K_m (μM)	Δ	k_{cat} (s^{-1})	Δ	K_m (mM)	Δ
wild-type	10.0 ± 0.5		56 ± 4		0.34 ± 0.09		8 ± 2	−
E187A	0.023 ± 0.002	400	88 ± 7	−	0.00053 ± 0.00004	600	13 ± 4	−
E187Q	0.009 ± 0.001	1000	86 ± 15	−	0.00044 ± 0.00006	800	17 ± 3	2↑
E187S	0.002 ± 0.001	5000	55 ± 54	−	0.00026 ± 0.00003	1300	14 ± 3	2↑
E187D	0.055 ± 0.003	200	24 ± 3	2↓	0.006 ± 0.001	60	59 ± 10	7↑

generation of the products G-3-P and DHAP was k_2. The rate constant k_2 represented only the carbon−carbon bond cleavage step since acid quench immediately releases product. Data were fit by an iterative method to equations derived from the model as described previously (*18*).

Superfamily Analysis. The three-dimensional structures of FBPA (1ADO), TRANS (1ONR), KDPGA (1EUA), DRPA (1JCJ), NAL (1NAL), DHDS (1QFE), and DQD (1DHP) were overlaid using the Web-based program COMPARER (www-cryst.bioc.cam.ac.uk/COMPARER) (*36*). The algorithm that was utilized is the least-squares alignment of the secondary structural elements identified from the crystallographic coordinates. The program also uses the alignment of the secondary structural elements to generate a JOY alignment of the primary sequence (*37*) from which the percent sequence identity was calculated. The pairwise percent sequence similarity was calculated using identity and similarity utilizing both PAM 250 and BLOSUM 62 matrices. The analysis was performed on two negative control groups of structures. One consisted of enzymes that share the α/β barrel fold but catalyze their reactions with different mechanisms and are thus not thought to be homologues [mandelate racemase (2MNR), xylose isomerase (1AOC), 5-aminolavulinic acid dehydratase (1YLV), triose phosphate isomerase (1AMK), tryptophan synthase (2TYS), and class II aldolase (1DOS)]. The second control group consisted of aldolase superfamily members in which the arrangement of α/β motifs was altered (circularly permutated). The routine lsq_explicit from the molecular graphics program O (*38*) was used to obtain the rmsd of the overlaid structures for the common atoms (those from the overlapping secondary structural elements). In all cases, the program lsq_explicit did not alter the alignment obtained from COMPARER.

RESULTS

Steady-State Kinetics of Mutant Proteins. The E187A, E187Q, E187S, and E187D substitutions in rabbit FBPA were created by site-directed mutagenesis and subcloned into a high-copy number plasmid for protein expression. Sequencing of the entire coding region confirmed the presence of the desired mutation without unintentional changes. Proteins were expressed in *E. coli* DH5α where up to 20% of total protein was the recombinant aldolase as shown by SDS−PAGE. The recombinant enzymes were purified by substrate affinity elution from CM-Sepharose with yields of purified protein (>95% pure as determined by SDS−PAGE) ranging between 15 and 170 mg/L of culture.

The ability of the substituted aldolases to cleave Fru-1,6-P_2 and Fru-1-P was assessed and revealed that the k_{cat} values for Glu187-substituted enzymes against Fru-1,6-P_2 were 200−5000-fold lower than that of wild-type FBPA, while the K_m values were approximately the same as that for the wild type (Table 2). The expectation for removal of the Glu187 carboxylate by the Ala substitution would be loss of acid/base chemistry; however, the vacated space might allow this functionality to come from a water molecule. Using the isosteric substitution with Gln and/or Ser tested this possibility, although the Ser might coordinate such a water molecule with some steric consequences. The substitution with Asp would restore the acid functionality but with a loss of proximity. E187A, which removed the carboxylate functionality, exhibited a 400-fold decrease in k_{cat}. The isosteric substitution, E187Q, produced a 1000-fold decrease in k_{cat}. Replacement of glutamate with a small polar side chain, E187S, yielded the lowest activity with a 5000-fold decrease in k_{cat}. Activity was recovered somewhat with the E187D substitution, which had the highest activity among the Glu187-substituted enzymes with an activity only 200-fold lower than that of the wild type. The kinetic constants against Fru-1-P were measured for the Glu187-substituted aldolases as well (Table 2) and showed k_{cat} and K_m values that mirrored those for Fru-1,6-P_2. The similar activity profiles toward either Fru-1,6-P_2 or Fru-1-P indicated that Glu187 is not involved in C6−phosphate binding. This interpretation is supported by the small effects of mutation on K_m values for either substrate.

Single-Turnover Analysis. The large k_{cat} effect only has meaning if the rate-limiting step can be discerned for each Glu187-substituted aldolase. Single-turnover experiments were therefore carried out with these substituted enzymes to determine if the substitution is involved in the rate-limiting step. Each aldolase was incubated with excess [U-^{14}C]Fru-1,6-P_2 followed by an acid quench. The covalently bound Schiff-base intermediates were precipitated with the protein, while noncovalently bound substrates and products were released into the supernatant fraction. As a function of time, the amount of remaining Fru-1,6-P_2, the amount of covalently bound substrate (measuring the extent of Schiff-base/carbinolamine formation), and the appearance of each triose product (measuring C3−C4 bond cleavage) were determined. This enabled measurement of the rate of Schiff-base formation by the incorporation of Fru-1,6-P_2 into the protein precipitate upon quenching with HCl and the depletion of [U-^{14}C]Fru-1,6-P_2 from the supernatant fraction. The rate of C3−C4 bond cleavage was measured by the generation of the product [^{14}C]trioses in the supernatant fraction after separation of the substrate and the two products by TLC. The wild-type aldolase A reaction was performed in a rapid-quench apparatus at 4 °C, and the mutant reactions were carried out at 22 °C either on the benchtop or in the rapid-quench apparatus on a long time scale.

The concentrations of covalent intermediates, remaining substrates, and products versus time were plotted and fit to equations for a two-step irreversible process. The plots of

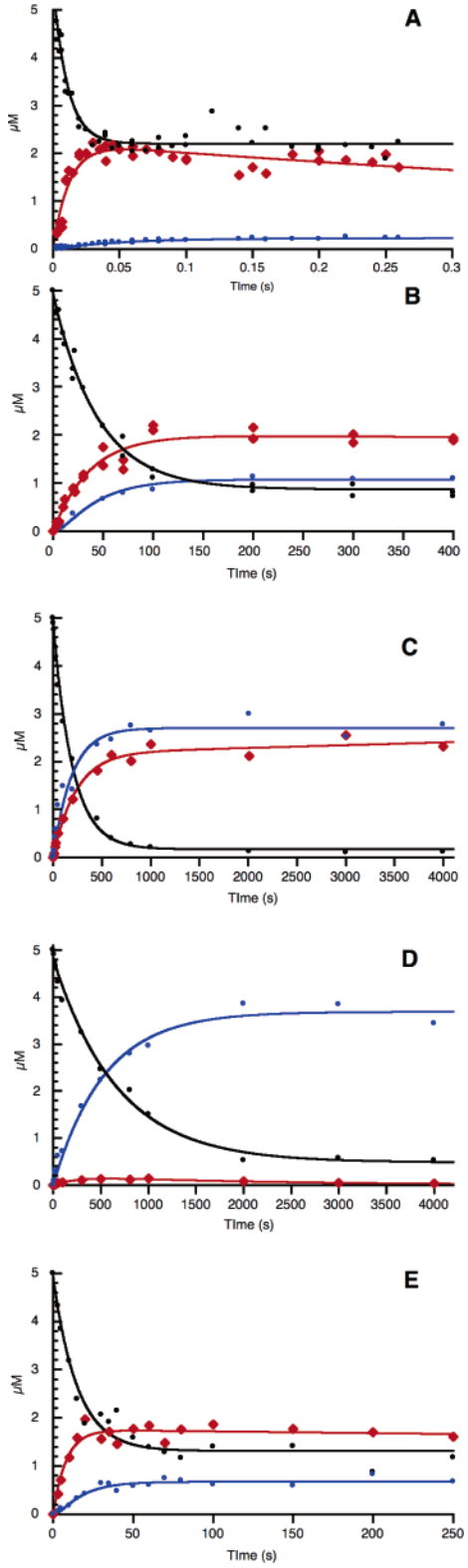

FIGURE 1: Single turnover in the forward reaction. A solution of [U-^{14}C]Fru-1,6-P_2 was mixed with a solution of enzyme to start the reaction with final concentrations of 5 and 65 μM, respectively. The remaining substrate (black, ●), covalent intermediates (red, ◆), and product release (blue, ●) were monitored. The curves were calculated as described in Materials and Methods: (A) wild-type enzyme, (B) E187A, (C) E187Q, (D) E187S, and (E) E187D.

wild-type enzyme and Glu187-substituted aldolases are shown in Figure 1. Rate constants were calculated from fitting the data to exponential equations based on a two-step kinetic model (Table 3). The apparent rate constant representing the rate of Schiff-base formation is k_1, and the rate of product generation, G-3-P and DHAP, is k_2. The rate constant k_2 represents only the carbon−carbon bond cleavage step since acid quench immediately releases both G-3-P and noncovalently bound DHAP. The rate of appearance of DHAP represents DHAP release and is rate-limiting for wild-type FBPA (*17*, *18*). Although in the wild-type enzyme, G-3-P is released prior to DHAP (*14*), there was no difference in the release of the two trioses for the Glu187-substituted aldolases. Thus, for the kinetic treatment described here, the apparent rate constant k_2 includes both products.

For wild-type FBPA, the formation of the Schiff base ($k_1 \sim 80$ s^{-1}) was faster than carbon bond cleavage ($k_2 \sim 30$ s^{-1}), and both were faster than k_{cat} (1 s^{-1}). All Glu187-substituted aldolases were able to form covalent intermediates, although with reduced rates (k_1 between 0.002 and 0.12 s^{-1}) at 22 °C. The most detrimental substitution was E187S, which produced a 55000-fold decrease in the level of Schiff-base formation compared to that of the wild type. E187S was followed by E187Q (16000-fold decrease), E187A (3000-fold decrease), and E187D (1000-fold decrease). These enzymes had the same relative fold decrease in the level of Schiff-base formation as they had in k_{cat}. With perhaps the exception of that of E187D, the k_1 values for the Glu187-substituted enzymes were not significantly different from one another whether they were determined from depletion of Fru-1,6-P_2 from the supernatant fraction or incorporation of Fru-1,6-P_2 into enzyme. The k_1 values of all the Glu187-substituted aldolases were equal to their respective k_{cat} values. This clearly indicates that carbinolamine or Schiff-base formation is partially rate-limiting for these enzymes and that Glu187 plays a pivotal role in Schiff-base formation.

Although the rates of Schiff-base formation were significantly decreased (1000−55000-fold) for Glu187-substituted enzymes, rates of C3−C4 bond cleavage were not affected as much, but these rates were deceiving. With the possible exception of E187A, and as expected for a reaction following one that is partially rate-limiting, the apparent rates of the subsequent step, carbon bond cleavage (k_2), in these enzymes were also approximating their respective k_{cat} values. The rate of C3−C4 bond cleavage (k_2) for both E187D and E187A was ~0.1 s^{-1}. This rate was 300-fold slower than the rate of carbon bond cleavage determined for the wild-type enzyme. However, this reduction in rate did not account for the decreased k_{cat} for these mutants since the carbon bond cleavage was still 5-fold faster than Schiff-base formation (as it is in wild-type FBPA). For the other substitutions, E187Q and E187S, k_2 could not be measured accurately when using a double-exponential equation with a fixed value of k_1. However, when the plot of the concentration of triose phosphates versus time was fit to the single exponential, the rate constant was found to be 0.0051 and 0.0018 s^{-1}, which is consistent with the k_{cat} (k_1) for each mutant. Furthermore, for the E187S enzyme, the Schiff-base intermediates clearly did not accumulate to the extent that they did for other mutants or the wild-type enzyme (see Figure 1D). This indicated that the formation of Schiff base and/or carbinolamine is now fully rate-limiting since there is no buildup of any covalent intermediates. Last, the fact that covalent intermediates accumulated on the enzyme means that subsequent steps are still relatively slow.

Table 3: Rate Constants from Single-Turnover Experiments

	Fru-1,6-P_2 Schiff-base intermediate formation			triose phosphate production			
aldolase	Fru-1,6-P_2 depletion k_1 (s^{-1})	Fru-1,6-P_2 incorporation k_1 (s^{-1})	Δ	Fru-1,6-P_2 cleavage k_2 (s^{-1})	Δ	k_{cat} (s^{-1})[b]	k_1:k_{cat}
wild-type[a]	82 ± 6	83 ± 10		31 ± 3		1	80
E187A	0.023 ± 0.0014	0.024 ± 0.0017	3000	0.096 ± 0.036	300	0.023	1
E187Q	0.0051 ± 0.0003	0.0043 ± 0.0006	16000	0.0051 ± 0.0005[c]	6000	0.009	0.6
E187S	0.0015 ± 0.0001	na[d]	55000	0.0018 ± 0.0002[c]	15000	0.002	0.8
E187D	0.060 ± 0.01	0.12 ± 0.022	1000	0.096 ± 0.021	300	0.055	1.1

[a] The wild type was assessed at 4 °C to slow the reaction sufficiently to measure rates; the Glu187 mutants were all assessed at 22 °C. Therefore, the fold changes from the wild-type values are likely underestimated. [b] From Table 2, except for that of the wild type, which was determined at 4 °C (*18*). [c] The value was calculated from a single exponential. [d] The value could not be calculated as there was negligible production of the Schiff-base intermediate.

The kinetic analyses of the site-directed mutants at Glu187 demonstrated a role in Schiff-base formation via dehydration of the carbinolamine or a role in hydration of the keto oxygen on attack of the carbonyl by the lysine. However, model reactions of imine formation have shown that this latter reaction does not require acid/base catalysis and the keto oxygen is protonated by an intramolecular migration from the attacking amino group (*39*), favoring the role of Glu187 in dehydration of the carbinolamine. Overall, the single-turnover kinetic results, together with previous mechanistic and structural results, support the role of the Glu187−Lys229 pair as a catalytic dyad required for catalysis of Schiff-base formation.

Superfamily Alignment. Schiff-base formation is a mechanistic strategy used by many enzymes. The possibility that homologous enzymes would utilize an additional residue for acid/base catalysis during Schiff-base formation, like Glu187 of FBPA, exists. All members of the family would possess this conserved catalytic dyad. If so, this acid/base residue should be contributed to the active site from the same element of secondary structure that was found for FBPA. In addition to other aldolases (KDPGA, DRPA, and TRANS), the NAL family of lyases also uses a Schiff-base intermediate (NAL, DQD, and DHDPS). A multiple primary sequence alignment of all seven of these enzymes does not show any significant similarity. Three-dimensional structural alignment was therefore used to detect homologous residues in a sequence alignment based on this structural overlay. As negative controls for the structure-based sequence alignment, the sequences of these enzymes were circularly permuted by renumbering the Protein Data Bank files such that secondary structural elements from the original barrel were now shifted relative to one another (i.e., the β1, β2, β3, β4, β5, β6, β7, β8 order now becomes β4, β5, β6, β7, β8, β1, β2, β3). A second control group of TIM barrel enzymes that were not mechanistically related to one another or to the aldolases was chosen. When this group of Schiff-base enzymes was overlaid, using the Web-based program COMPARER, there was significant identity. The alignment of the two blocks of sequence around the fifth and sixth β-strands, from which the catalytic dyad residues corresponding to Glu187 and Lys229 of FBPA, respectively, are contributed, is shown in Figure 2. The Schiff-base lysine from the sixth β-strand aligned identically for all enzymes. The other member of the catalytic dyad, contributed from the fifth β-strand, was Tyr from NAL and DHDPS, Glu from FBPA and TRANS, and His from DQD (displaced by two residues). A glutamate from KDPGA previously suggested to play this role (*40*) is

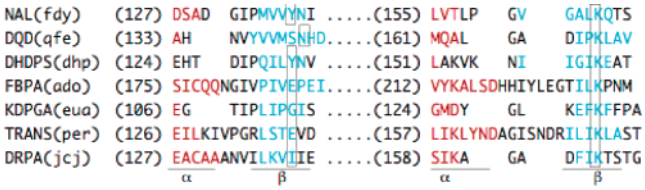

FIGURE 2: Sequence alignment of the class I aldolase superfamily. A partial primary sequence alignment taken from the output of COMPARER is depicted showing the blocks of sequence around β-strands 5 (left) and 6 (right). The FBPA Glu187 and Lys229 residues, along with the analogous residues in the other enzymes, are boxed, and these two residues comprise the catalytic dyad. Red lettering denotes those residues found in an α-helix, and cyan denotes those residues in a β-strand. The acid catalysts for KDPGA and DRPA do not lie in the same β-strand (see Table 1).

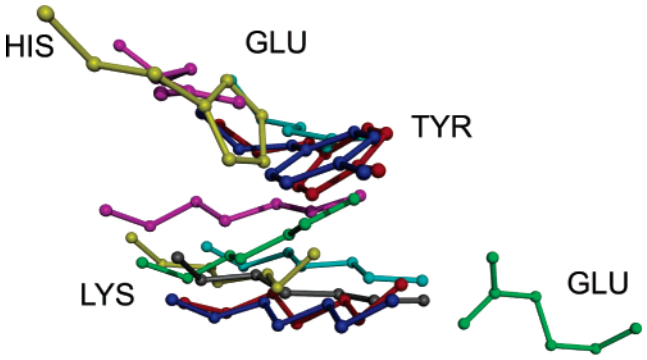

FIGURE 3: Catalytic dyad of the aldolase superfamily. The multiple-protein alignment was used to optimize the relationships of the secondary structure elements and minimize the rmsd. The Schiff-base-forming lysine and the general acid assisting in dehydration of the carbinolamine (except for DRPA, which uses a water molecule) are depicted. NAL is colored red. DQD is colored yellow. DHDPS is colored blue. FBPA is colored cyan. KDPGA is colored green. DRPA aldolase is colored gray. TRANS is colored purple.

contributed from a different β-strand (β2). This, however, indicates that this Glu may play a different role (if any) and that the catalytic dyad in KDPG may comprise the Lys and a water as it does for DRPA (*41*). The superimposition of these catalytic dyad residues is shown in Figure 3. This overlay clearly shows that Glu, Tyr, and His residues occupy the same relative positions in their respective active sites.

Given that some of the levels of pairwise identity based on the primary sequence alignment among the established NAL family members (*10*) were low (16−19%), the levels of pairwise identity among members of the expanded superfamily were not expected to be great. The entire alignment generated by COMPARER (displayed in JOY format) was used to calculate the level of pairwise sequence

Table 4: Percent Identity of the Aldolase Superfamily

	NAL	DQD	DHDPS	FBPA	KDPGA	TRANS	DRPA
NAL	100						
DQD	27[a]	100					
DHDPS	11[a]	13[a]	100				
FBPA	13	6	8	100			
KDPGA	13	10	16	14	100		
TRANS	12	11	13	9	13	100	
DRPA	13	11	12	12	15	9	100

[a] From the NAL family.

identity among these seven enzymes (Table 4). The NAL family had an even broader range (11−27%) of similarity in the JOY alignment, which is based on the tertiary structures, than one based on the primary sequence alone. The 27% level of pairwise identity between NAL and DQD suggests that these two enzymes may have a closer evolutionary relationship than NAL or DHDPS has to the other members of the superfamily. Most of the levels of pairwise identity among the superfamily members were in the same range as the lower values among the NAL family (11−13%). In fact, the average level of identity calculated from the 21 pairs (12 ± 4%) was in this range. This average was compared either to the permuted structures using the sequences of the seven enzymes (11 ± 2%) or to the average levels of pairwise identity among six random $(\alpha/\beta)_8$ barrel enzymes (10 ± 2%). The significance test of the percentage identity among all seven proteins compared to the permuted proteins was in a low confidence interval ($p = 0.2$); however, compared to the six random $(\alpha/\beta)_8$ barrel enzymes, it was at a high confidence interval ($p = 0.005$). Furthermore, when the BLOSUM matrix was applied to the alignments to calculate the degree of sequence similarity, the aldolase family was 24 ± 6% similar, the permuted group was 21 ± 3% similar, and the six random $(\alpha/\beta)_8$ barrel enzymes were 22 ± 6% similar. The confidence intervals for a significant difference between the aldolase family and either the permuted proteins ($p = 0.025$) or the six random $(\alpha/\beta)_8$ barrel enzymes ($p = 0.002$) were greater than the comparison of the levels of identity. This overall similarity among this group of Schiff-base enzymes and the conservation of a catalytic dyad indicated that all these enzymes were homologous. This conclusion was supported by a similar analysis of the rmsd and pairwise *z*-scores among the family members compared to the six random $(\alpha/\beta)_8$ barrel enzymes (data not shown).

DISCUSSION

Understanding evolutionary relationships among enzymes sharing the $(\alpha/\beta)_8$ barrel fold is challenging due to the high frequency of this fold (*42*). Some seemingly conserved residues might be intimately linked to formation of the fold itself, and these might not represent a common ancestry. Thus, mechanistically related enzymes that may apparently have evolved by divergent evolution may instead have evolved by convergent evolution to a common mechanism. The possibilities of convergent and divergent evolution may be distinguished if enzymes within the mechanistically diverse superfamily (1) share a greater level of sequence identity than mechanistically unrelated enzymes with the same fold and (2) possess essential catalytic residues that are stationed on the same secondary structural elements within the fold (*19*). To undertake such an analysis in the aldolase superfamily, it is first essential to delineate any additional residues beyond the Schiff-base-forming lysine that would represent the common chemistry employed in this superfamily.

Structures of the FBPA−DHAP and FBPA−Fru-1,6-P_2 Schiff base have been previously determined by X-ray crystallography by trapping the catalytic intermediate with $NaBH_4$ or cryogenically in the presence of Fru-1,6-P_2 (*20*, *25*). In these structures, the position of Glu187 in relation to the DHAP Schiff base is consistent with a role for this residue in protonation of the hydroxyl group of the carbinolamine in the dehydration step, thus catalyzing Schiff-base formation. The possibility of a role for Glu187 in Schiff-base chemistry suggested that it might be utilized in other Schiff-base enzymes. The overlay of the FBPA−DHAP structure with those of the covalent enzyme−dihydroxyacetone structure of the mechanistically similar TRANS and enzyme−carbinolamine structure of KDPGA allowed the identification of a conserved Lys−Glu dyad involved in three Schiff-base-forming aldolases (Glu187, Glu96, and Glu45, respectively) (*20*). The structural overlay of these two residues in mechanistically related enzymes suggested the possibility of a conserved role for the dyad in enzyme-catalyzed Schiff-base chemistry. The structural evidence is supported by kinetic evidence for the role of the second member of the catalytic dyad acting as a general acid/base catalyst in Schiff-base formation and breakdown. Substitutions of the general acid base residue in TRANS (E96A), DHDPS (Y133F), NAL (Y133F), and DQD (H143A) produce changes in catalysis similar to those of the corresponding mutation in FBPA (E187A), with 25−400-fold changes in k_{cat} and little to no change in K_m (the exception to this is NAL in which there is also a 100-fold increase in K_m) (*43*−*46*). X-ray crystallographic structures of E96A TRANS and Y133F DHDPS showed, as for E187A and E187Q FBPA (*27*), that side-chain replacement did not induce unanticipated structural changes in the substituted enzymes; changes were localized to the site of replacement. In addition, H143A DQD exhibited accumulation of the product Schiff base at the active site (identified by electrospray ionization mass spectrometry) at a rate similar to the turnover rate of the mutant enzyme (*45*). Together, all evidence is consistent with the role of the second residue of the catalytic dyad acting as a general acid in the formation of the imine intermediate and as a general base in Schiff-base hydrolysis. In this study, this catalytic role of Glu187 of FBPA was investigated by site-directed mutagenesis coupled with steady-state and pre-steady-state kinetics.

The dramatic loss of activity in Glu187-substituted enzymes (200−5000-fold in k_{cat} for Fru1,6-P_2) strongly suggests a role for the glutamic acid in catalysis. The comparable effect of the Glu187 mutation on k_{cat} with either Fru-1,6-P_2 or Fru-1-P as a substrate indicates that the role of Glu187 lies in the common chemistry for both substrates. Also, none of the substitutions considerably altered the K_m of the enzyme toward either Fru-1,6-P_2 or Fru-1-P, suggesting that Glu187 does not participate in hexose binding. Replacement of Glu187 with Asp had the least detrimental effect (200-fold decrease) among the four substitutions, suggesting the carboxylate of Glu is critical but that positioning effects are also important. Comparison with the Gln substitution, which produced a 1000-fold decrease in k_{cat}, also supports this

conclusion. In addition, the E187Q-substituted enzyme was one of two X-ray crystallographic structures of Glu187-substituted enzymes previously reported (*27*; PDB entry 1EWG). These structures showed that these substitutions did not cause significant alteration of the active-site structure. Surprisingly, substitution with Ala was less detrimental to the enzyme than substitution with Gln, resulting in an only 400-fold decrease in k_{cat}. This effect was unexpected. However, if Glu187 acts as an acid/base catalyst, then substitution with bulky, neutral residues would severely compromise this role, whereas the small size of Ala may permit substitution by a water molecule to take on the role of the Glu carboxylate. The structure of E187A (PDB entry 1EX5) shows that indeed there are no major changes in overall architecture (rmsd from the wild type of 0.73 Å^2) or active-site structure due to the mutation (*27*). The enzyme displaying the lowest activity, E187S (5000-fold decrease in activity), is intriguing. It is not clear why this mutation has a more adverse effect than other substitutions. Since the measured k_1 includes steps from substrate binding through carbinolamine formation, E187S may affect one of these intermediate steps, which is invisible in the kinetics of the other substituted enzymes. The Schiff-base formation and carbon−carbon bond cleavage occurred at the same rate (see Table 3). Most notably, covalent intermediates did not build up in this enzyme (see Figure 1), suggesting that Schiff-base formation is rate-limiting for the E187S substitution and subsequent reactions occurred more rapidly. In contrast, the E187Q substitution produced similar relative rates but revealed a buildup of covalent intermediates following carbon−carbon bond cleavage. The partially rate-limiting step of Schiff-base formation followed by a buildup of covalent intermediates indicates that these intermediates are likely bound DHAP. This phenomenon connotes the possibility that the Ser more effectively catalyzes the breakdown of covalent intermediates in the reverse direction.

Previously, mechanistic proposals for the role of Glu187 include maintenance of a neutral electrostatic potential at the active site (*27*, *47*), a proton acceptor from the nitrogen atom of the carbinolamine intermediate (*48*), a proton donor to the carbonyl group of the substrate in carbinolamine formation (*48*), participation in proton transfer in the dehydration step of the carbinolamine (*25*, *49*), and a proton acceptor from the C4 hydroxyl initiating carbon−carbon bond cleavage (*25*, *27*). The large decrease in the rate of formation of the intermediate in pre-steady-state kinetics is consistent with any and all of these roles. Recent structures captured FBPA in the Schiff-base form, in a ground-state complex with the substrate analogue tagatose bisphosphate (*25*), and in the carbinolamine form of an archaeal FBPA (*26*). The former structure (*25*) has been used to support a role for Glu187 in both Schiff-base chemistry and proton removal at the C4 hydroxyl associated with carbon−carbon bond cleavage. The proposal is based on the position of the Glu187 side chain with respect to the substrate analogue and intermediate. This finding highlights the importance of the Glu−Lys dyad. However, in the structure of FBPA complexed with Fru-1,6-P_2 from archaebacteria, which had the residue analogous to Glu187 (Tyr146) substituted with Phe (Y146F), a carbinolamine with Fru-1,6-P_2 was trapped. This structure indicated that (1) residues other than Glu originating from β-strand 5 can serve as acid catalysts, as in DHDPS, NAL, and DQD, and (2) these residues in the aldolase superfamily most likely catalyze the dehydration of the carbinolamine. This is further supported by functional evidence from single-turnover kinetics presented herein, which demonstrated that in all the Glu187-substituted enzymes, Schiff-base formation is rate-limiting or partially rate-limiting. Furthermore, it is notable that the kinetic data do not completely support the notion that Glu187 could act as the catalytic base for carbon−carbon bond cleavage. In both the E187A and E187D enzymes, the rates of Schiff-base formation and Fru-1,6-P_2 cleavage are not affected to the same extent. Namely, the rate of carbon−carbon bond cleavage is slowed less than the rate of Schiff-base formation relative to that of wild-type FBPA (a 300−6000-fold decrease vs a 3000−16000-fold decrease). Moreover, for these two substituted enzymes, the rates of Schiff-base intermediate formation equal k_{cat}, while the rates of carbon−carbon bond cleavage do not (although the C−C bond cleavage rates are indeed reduced in these mutants compared to that of the wild-type enzyme). Whether the role of Glu187 encompasses the carbon−carbon bond cleavage step, all available evidence is consistent with an essential acid/base role for this residue (and its equivalents in superfamily homologues) in Schiff-base chemistry.

The class I fructose-6-phosphate aldolase was reportedly related to the transaldolases (*50*) and, like TRANS, has a two-stranded circular permutation of the barrel. The X-ray crystallographic structure of this enzyme reveals the use of an ordered water molecule for catalysis of Schiff-base formation, similar to that of DRPA. This water forms a hydrogen bond to Gln59, which is contributed from a strand corresponding to β-strand 5 in the permuted structure, and aligns among the transaldolases with the Glu96 that has been implicated in Schiff-base formation (*43*, *50*). The alternate use of a structurally ordered water molecule as well as different residues to catalyze Schiff-base formation exemplifies the different modes for catalyzing this step in Schiff-base enzymes.

The superimposition of the superfamily members using their three-dimensional structures leads to sequence alignment, which shows a statistically significant difference in percent identity from mechanistically unrelated enzymes sharing the common α/β barrel fold. This overlay clearly shows that the Schiff-base lysine and second residue of the catalytic dyad (Glu, Tyr, or His) occupy the same positions in the enzymes' respective active sites. Salient to this point, a common directionality of the Schiff-base stereochemistry can be noted among the superfamily members (see Table 1). In all cases, a *si*-face attack is inferred from the configuration of the resulting (*R*)-carbinolamine or from the resulting reduced lysines in the X-ray crystallographic structures of available family members. Thus, both the elements of secondary structure stationing the catalytic dyad and the binding orientation of the substrate (and thus the stereochemistry of the resulting reaction) have been retained throughout evolution of the family.

In contrast to the conservation of the location and directionality of the catalytic dyad among family members, it appears that the location of the key base that initiates carbon−carbon bond cleavage among the aldolase superfamily members is not well conserved. For FBPA, Asp33 and Lys146, implicated in this step (*18*, *20*, *22*), are

contributed by β-strands 1 and 4, respectively. For TRANS, Asp17 is stationed on permutated β-strand 3. For KDPGA, Glu45 is contributed by β-strand 2. It may be of interest that the Glu45 in β-strand 2 of KDPGA aligns with Cys47, Glu46, and Tyr43 residues in DRPA, NAL, and DQD, respectively. Although the key base has not been identified in these enzymes, these residues are in the active site proximal to the Schiff-base lysine. While it has been reported for DRPA that an ordered water molecule is used as the key base, it is liganded by Cys47 (β-strand 2), along with Asp16, Thr18 (β-strand 1), and Asp102 (β-strand 4) (*41*). The apparent lack of conservation of the key base residue identity and position indicates that the evolution of the key base is an adaptation of these enzymes for their particular substrates; thus, different key base residues were utilized by each family member.

If, as it has been suggested (*25*), Glu187 in addition to participating in Schiff-base chemistry plays the role of abstracting the proton from O4 during C−C bond cleavage, then Glu187 and its equivalents identified herein may play a universal role in acid/base catalysis in the mechanism of the class I aldolase family. Future structural and biochemical studies of these and new members of the family should confirm the essential nature of the catalytic dyad and the phylogenetic relationship between these enzymes.

The structural and mechanistic analyses provided herein have uncovered (1) the existence and importance to catalysis of a catalytic dyad in a superfamily of enzymes that utilize Schiff-base chemistry, (2) significant identity among aldolase superfamily members, and (3) a common use of directionality during catalysis by the catalytic dyad. Together, these results confirm the difficult assignment of a group of enzymes with a commonly used fold as related by divergent evolution. Intriguing is the observation of the variation in residues used as the second member of the catalytic dyad and the ability to utilize a water molecule instead. This variation underscores the plasticity in the α/β barrel active site in evolving to accommodate substrates of different geometry, size, and charge.

ACKNOWLEDGMENT

We thank Drs. Nicholas Silvaggi and John A. Pezza for helpful discussions and critical review of the manuscript.

REFERENCES

1. Neidhart, D. J., Kenyon, G. L., Gerlt, J. A., and Petsko, G. A. (1990) Mandelate racemase and muconate lactonizing enzyme are mechanistically distinct and structurally homologous, *Nature 347*, 692−694.
2. Babbitt, P. C., and Gerlt, J. A. (1997) Understanding enzyme superfamilies. Chemistry as the fundamental determinant in the evolution of new catalytic activities, *J. Biol. Chem. 272*, 30591−30594.
3. Gerlt, J. A., and Babbitt, P. C. (2000) Can sequence determine function? *Genome Biol. 1*, REVIEWS0005.1−REVIEWS0005.9.
4. Murzin, A. G., Brenner, S. E., Hubbard, T., and Chothia, C. (1995) SCOP: A structural classification of proteins database for the investigation of sequences and structures, *J. Mol. Biol. 247*, 536−540.
5. Rutter, W. J. (1960) Aldolase, *Enzymes 5*, 341−372.
6. Horecker, B. L., Tsolas, O., and Lai, C. Y. (1975) Aldolases, in *The Enzymes* (Boyer, P. D., Ed.) pp 213−258, Academic Press, New York.
7. Marsh, J. J., and Lebherz, H. G. (1992) Fructose-bisphosphate aldolases: An evolutionary history, *Trends Biochem. Sci. 17*, 110−113.
8. Cooper, S. J., Leonard, G. A., McSweeney, S. M., Thompson, A. W., Naismith, J. H., Qamar, S., Plater, A., Berry, A., and Hunter, W. N. (1996) The crystal structure of a class II fructose-1,6-bisphosphate aldolase shows a novel binuclear metal-binding active site embedded in a familiar fold, *Structure 4*, 1303−1315.
9. Sygusch, J., Beaudry, D., and Allaire, M. (1987) Molecular architecture of rabbit skeletal muscle aldolase at 2.7-Å resolution, *Proc. Natl. Acad. Sci. U.S.A. 84*, 7846−7850.
10. Lawrence, M. C., Barbosa, J. A., Smith, B. J., Hall, N. E., Pilling, P. A., Ooi, H. C., and Marcuccio, S. M. (1997) Structure and mechanism of a sub-family of enzymes related to *N*-acetylneuraminate lyase, *J. Mol. Biol. 266*, 381−399.
11. Barbosa, J. A., Smith, B. J., DeGori, R., Ooi, H. C., Marcuccio, S. M., Campi, E. M., Jackson, W. R., Brossmer, R., Sommer, M., and Lawrence, M. C. (2000) Active site modulation in the *N*-acetylneuraminate lyase sub-family as revealed by the structure of the inhibitor-complexed *Haemophilus influenzae* enzyme, *J. Mol. Biol. 303*, 405−421.
12. Grazi, E., Rowley, P. T., Chang, T., Tchola, O., and Horecker, B. L. (1962) The mechanisms of action of aldolases III: Schiff base formation with lysine, *Biochem. Biophys. Res. Commun. 9*, 38−43.
13. Midelfort, C. F., Gupta, R. K., and Rose, I. A. (1976) Fructose 1,6-bisphosphate: Isomeric composition, kinetics, and substrate specificity for the aldolases, *Biochemistry 15*, 2178−2185.
14. Rose, I. A., O'Connell, E. L., and Mehler, A. H. (1965) Mechanism of the aldolase reaction, *J. Biol. Chem. 240*, 1758−1765.
15. Rose, I. A., and Warms, J. V. B. (1985) Complexes of muscle aldolase in equilibrium with fructose 1,6-bisphosphate, *Biochemistry 24*, 3952−3957.
16. Choi, K.-H., and Tolan, D. R. (2004) Presteady-state kinetic evidence for a ring-opening activity in fructose-1,6-(bis)phosphate aldolase, *J. Am. Chem. Soc. 126*, 3402−3403.
17. Rose, I. A., Warms, J. V. B., and Kuo, D. J. (1987) Concentration and partitioning of intermediates in the fructose bisphosphate aldolase reaction. Comparison of the muscle and liver enzymes, *J. Biol. Chem. 262*, 692−701.
18. Morris, A. J., and Tolan, D. R. (1994) Lysine-146 of rabbit muscle aldolase is essential for cleavage and condensation of the C3−C4 bond of fructose 1,6-bis(phosphate), *Biochemistry 33*, 12291−12297.
19. Matthews, B. W., Remington, S. J., Grutter, M. G., and Anderson, W. F. (1981) Relation between hen egg white lysozyme and bacteriophage T4 lysozyme: Evolutionary implications, *J. Mol. Biol. 147*, 545−558.
20. Choi, K. H., Shi, J., Hopkins, C. E., Tolan, D. R., and Allen, K. N. (2001) Snapshots of catalysis: The structure of fructose-1,6-(bis)phosphate aldolase covalently bound to the substrate dihydroxyacetone phosphate, *Biochemistry 40*, 13868−13875.
21. Choi, K. H., Mazurkie, A. S., Morris, A. J., Utheza, D., Tolan, D. R., and Allen, K. N. (1999) Structure of a fructose-1,6-bis-(phosphate) aldolase liganded to its natural substrate in a cleavage-defective mutant at 2.3 Å, *Biochemistry 38*, 12655−12664.
22. Morris, A. J., and Tolan, D. R. (1993) Site-directed mutagenesis identifies aspartate 33 as a previously unidentified critical residue in the catalytic mechanism of rabbit aldolase A, *J. Biol. Chem. 268*, 1095−1100.
23. Morris, A. J., Davenport, R. C., and Tolan, D. R. (1996) A lysine to arginine substitution at position 146 of rabbit aldolase A shifts the rate-determining step to Schiff base formation, *Protein Eng. 9*, 61−67.
24. Blom, N., and Sygusch, J. (1997) Product binding and role of the C-terminal region in class I D-fructose 1,6-bisphosphate aldolase, *Nat. Struct. Biol. 4*, 36−39.
25. St-Jean, M., Lafrance-Vanasse, J., Liotard, B., and Sygusch, J. (2005) High-resolution reaction intermediates of rabbit muscle fructose-1,6-bisphosphate aldolase: Substrate cleavage and induced fit, *J. Biol. Chem. 280*, 27262−27270.
26. Lorentzen, E., Pohl, E., Zwart, P., Stark, A., Russell, R. B., Knura, T., Hensel, R., and Siebers, B. (2003) Crystal structure of an archaeal class I aldolase and the evolution of $(\beta/\alpha)_8$ barrel proteins, *J. Biol. Chem. 278*, 47253−47260.
27. Maurady, A., Zdanov, A., de Moissac, D., Beaudry, D., and Sygusch, J. (2002) A conserved glutamate residue exhibits multifunctional catalytic roles in D-fructose-1,6-bisphosphate aldolases, *J. Biol. Chem. 277*, 9474−9483.

28. Gilson, E., Clement, J. M., Brutlag, D., and Hofnung, M. (1984) A family of dispersed repetitive extragenic palindromic DNA sequences in *E. coli*, *EMBO J. 3*, 1417−1412.
29. Sayers, J. R., and Eckstein, F. (1989) Site-directed mutagenesis, based on the phosphorothioate approach, in *Protein Function* (Creigton, T. E., Ed.) pp 279−295, IRL Press, Oxford, England.
30. Beernink, P. T., and Tolan, D. R. (1992) Construction of a high-copy "ATG vector" for expression in *Escherichia coli*, *Protein Expression Purif. 3*, 332−336.
31. Hanahan, D. (1983) Studies on transformation of *Escherichia coli* with plasmids, *J. Mol. Biol. 166*, 557−580.
32. Racker, E. (1947) Spectrophotometric measurement of hexokinase and phosphohexokinase activity, *J. Biol. Chem. 167*, 843−854.
33. Cleland, W. W. (1990) Steady-state kinetics, *Enzymes 19*, 99−158.
34. Baranowski, T., and Niederland, T. R. (1949) Aldolase activity of myogen A, *J. Biol. Chem. 180*, 543−551.
35. Kuo, D. J., and Rose, I. A. (1985) Chemical trapping of complexes of dihydroxyacetone phosphate with muscle fructose-1,6-bisphosphate aldolase, *Biochemistry 24*, 3947−3952.
36. Sali, A., and Blundell, T. L. (1990) Definition of general topological equivalence in protein structures. A procedure involving comparison of properties and relationships through simulated annealing and dynamic programming, *J. Mol. Biol. 212*, 403−428.
37. Mizuguchi, K., Deane, C. M., Blundell, T. L., Johnson, M. S., and Overington, J. P. (1998) JOY: Protein sequence-structure representation and analysis, *Bioinformatics 14*, 617−623.
38. Jones, T. A., Zou, J. Y., Cowan, S. W., and Kjeldgaard, M. (1991) Improved methods for building protein models in electron density maps and the location of errors in these methods, *Acta Crystallogr. A47*, 110−119.
39. Sayer, J. M., Pinsky, B., Schonbrunn, A., and Washtien, W. (1974) Mechanism of carbinolamine formation, *J. Am. Chem. Soc. 96*, 7998−8009.
40. Allard, J., Grochulski, P., and Sygusch, J. (2001) Covalent intermediate trapped in 2-keto-3-deoxy-6-phosphogluconate (KDPG) aldolase structure at 1.95-Å resolution, *Proc. Natl. Acad. Sci. U.S.A. 98*, 3679−3684.
41. Heine, A., DeSantis, G., Luz, J. G., Mitchell, M., Wong, C. H., and Wilson, I. A. (2001) Observation of covalent intermediates in an enzyme mechanism at atomic resolution, *Science 294*, 369−374.
42. Hartmann, M., Schneider, T. R., Pfeil, A., Heinrich, G., Lipscomb, W. N., and Braus, G. H. (2003) Evolution of feedback-inhibited β/α barrel isoenzymes by gene duplication and a single mutation, *Proc. Natl. Acad. Sci. U.S.A. 100*, 862−867.
43. Schorken, U., Thorell, S., Schurmann, M., Jia, J., Sprenger, G. A., and Schneider, G. (2001) Identification of catalytically important residues in the active site of *Escherichia coli* transaldolase, *Eur. J. Biochem. 268*, 2408−2415.
44. Dobson, R. C., Valegard, K., and Gerrard, J. A. (2004) The crystal structure of three site-directed mutants of *Escherichia coli* dihydrodipicolinate synthase: Further evidence for a catalytic triad, *J. Mol. Biol. 338*, 329−339.
45. Leech, A. P., James, R., Coggins, J. R., and Kleanthous, C. (1995) Mutagenesis of active site residues in type I dehydroquinase from *Escherichia coli*. Stalled catalysis in a histidine to alanine mutant, *J. Biol. Chem. 270*, 25827−25836.
46. Kruger, D., Schauer, R., and Traving, C. (2001) Characterization and mutagenesis of the recombinant *N*-acetylneuraminate lyase from *Clostridium perfringens*: Insights into the reaction mechanism, *Eur. J. Biochem. 268*, 3831−3839.
47. Littlechild, J., and Watson, H. (1993) A data-based reaction mechanism for type I fructose bisphosphate aldolase, *Trends Biochem. Sci. 18*, 36−39.
48. Gefflaut, T., Blonski, C., Perie, J., and Willson, M. (1995) Class I aldolases: Substrate specificity, mechanism, inhibitors and structural aspects, *Prog. Biophys. Mol. Biol. 63*, 301−340.
49. Blonski, C., De Moissac, D., Perie, J., and Sygusch, J. (1997) Inhibition of rabbit muscle aldolase by phosphorylated aromatic compounds, *Biochem. J. 323*, 71−77.
50. Thorell, S., Schurmann, M., Sprenger, G. A., and Schneider, G. (2002) Crystal structure of decameric fructose-6-phosphate aldolase from *Escherichia coli* reveals inter-subunit helix swapping as a structural basis for assembly differences in the transaldolase family, *J. Mol. Biol. 319*, 161−171.
51. Trombetta, G., Balboni, G., di Iasio, A., and Grazi, E. (1977) On the stereospecific reduction of the aldolase-fructose 1,6-bisphosphate complex by $NaBH_4$, *Biochem. Biophys. Res. Commun. 74*, 1297−1301.
52. Jia, J., Huang, W., Schorken, U., Sahm, H., Sprenger, G. A., Lindqvist, Y., and Schneider, G. (1996) Crystal structure of transaldolase B from *Escherichia coli* suggests a circular permutation of the α/β barrel within the class I aldolase family, *Structure 4*, 715−724.

BI060239D